31st Annual International Conference of the IEEE EMBS
Minneapolis, Minnesota, USA, September 2-6, 2009

New Vectorcardiographic Non-planarity Measure of T-wave loop Improves Separation between Healthy Subjects and Myocardial Infarction Patients

Mari Karsikas, Kai Noponen, Heikki Huikuri, Tapio Seppänen

Abstract—**Principal component analysis of vectorcardiographic T-wave loop has been shown to be a potential tool to describe the abnormality of the cardiac repolarization and to predict cardiac events in patients with cardiac disease. In this paper a new method for estimating the non-planarity of the T-wave loop is introduced and tested with healthy subjects and subjects with anterior or inferior myocardial infarction. The method is based on the resamping of T-wave data points with respect to the arc-length, the total least squares plane fitting, the identifying and reordering of the fitted axes, and decomposing the optimal rotation matrix. A recently published related measure, PCA3, was used for comparison purposes. The results showed that the non-planarity of T-wave loop increased significantly in patients with myocardial infarction compared to the healthy group. The new method separated healthy and patient groups with p-value 0.002 while PCA3 only with p-value 0.075. The new method was superior to PCA3 in separating the healthy patients from both infarction types.**

I. INTRODUCTION

Principal component analysis (PCA) of the T-wave applied to 12-lead electrocardiograms (ECG) has been proposed as an approach to study the heterogeneity of repolarization without the need to determine the end of T-wave [1,2,3]. PCA has shown to be a more accurate and clinically useful surface ECG marker of the complexity of the repolarization than simple scalar intervals from the ECG, such as QTd [2]. Different ECG parameters obtained using PCA analysis, such as the QRS-T angle, PCA-ratio and the T-wave residuum have been associated among others with sudden cardiac death after myocardial infarction (MI) [4,5,6].

The PCA ratio is an old vectocardiographic (VCG) parameter that describes the T-wave loop roundness and it can be visualized by analogy as the long and short axes of the three-dimensional plane-like T-wave loop [7,8], see Fig.1b. In fact, the shape of the T-wave loop is not fully plane-like, but it also includes energy in the third orthogonal direction (see Fig.1c). However, the significance of the non-planarity has been paid only little attention to in previous studies. This may partly due to historical reasons: the degree of non-planarity, contrary to PCA-ratio, was not possible to calculate from the traditional two-dimensional projections of VCG loops in the time before digital signals.

To our knowledge, only Badilini *et al.* and Acar *et al.* have reported measures of the planarity of T-wave loop in their works in late 90's [9,10]. Specifically, the parameter PCA3 by Acar quantifies the projection of T-wave loop on a two dimensional plane spanned by the first and the third component. However, the published measures are sensitive to segmentation of T-wave from the ECG and to noise and other external influences such as movement artifacts.

The aims of the paper are:

1) to introduce a more robust technique to determine the non-planarity of VCG loop structures; and
2) to investigate how the non-planarity of the T-wave loop constructed by our new method works as a diagnostic value between healthy group and patients with anterior and inferior MI (see Fig. 1a.) compared to PCA3.

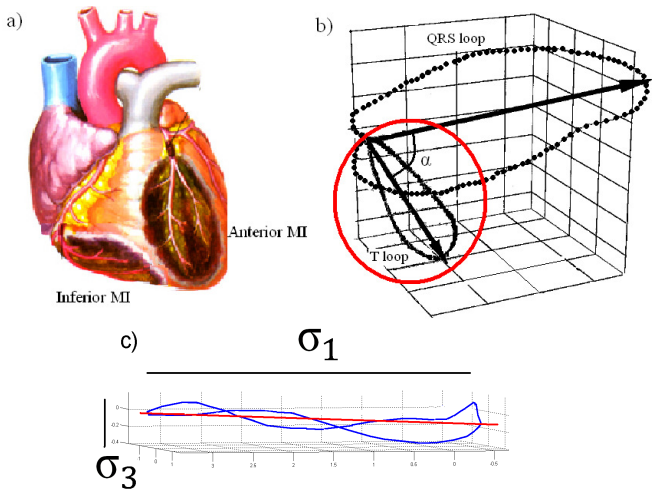

Figure 1. a) The locations of the anterior and inferior myocardial infarctions in a human's heart. b) The visualization of the T-wave loop in a PCA space. c) Illustration of the planarity of the T-wave loop (blue line). PCA3 measures the ratio between third end first eigenvalue.

II. METHODS

The analysis window of 12-lead ECG beat was defined to start in the middle of the iso-electric section before the QRS complex and to end in the next corresponding location. A

Manuscript received April 23, 2009.
M. Karsikas, K. Noponen, and T. Seppänen are with the Department Electrical and Information Engineering, Computer Engineering Laboratory PO BOX 4500, 90014 University of Oulu, FINLAND (e-mail: {mari.karsikas, kai.noponen, tapio.seppanen}@ee.oulu.fi)
H. Huikuri is with the Division of Cardiology, Department of Medicine, University Hospital of Oulu, PL 10, 90029 OYS, FINLAND (e-mail: heikki.huikuri@ppshp.fi)

linear baseline fit was estimated from the start and end points and subtracted from the signal. PCA was calculated using Singular Value Decomposition (SVD). The morphology analysis was carried out with our custom made QRS- and T-wave analysis software.

A. Non-planarity measure of T-wave loop

The proposed new method for estimating the three dimensionality of the loop structure is comprised of the following stages. First, the VCG is resampled with respect to the arc-length to obtain equidistantly placed points on both the QRS- and T-wave loop structures. Second, a total least squares plane fit is made to yield global information on the orientation of the loop structures. Third, the fitted axes are indentified and reordered based on behavior in time to correspond with the natural interpretation. Then, an optimal rotation matrix relating the two axis systems is estimated. Finally, the optimal rotation matrix is decomposed into Euler angles, and features describing the shape of the loop structure are calculated. These steps are described in the following subsections 1-6. However, a more detailed description of the initial part of the algorithm can be found in [11].

1) Arc-Length Resampling

In order to resample the data equidistantly with respect to arc-length

$$L(u) = \int_0^u \left|\frac{d\bar{r}}{dt}\right| dt, \quad (1)$$

we first construct a Piecewise Cubic Hermite Interpolating Polynomial (PCHIP) [12] fit for each of the leads. PCHIP retains the monotonicity of the data, and thus, no loops are formed to the VCG representations.

The inverse of the arc-length integral (1) is solved numerically using translated Gaussian quadrature rule [13], which reduces to evaluating the weighted sum of the PCHIP values at predetermined points. The exact equidistant points are then found by Newton's method iterating until sufficient resolution is achieved.

2) Fitting the Plane

A Total Least Squares (TLS) plane fit is made to the 3D vectorcardiografic data points $\bar{x}_i$. The fit minimizes

$$D = \sum_{i=1}^{M} (\bar{x}_i - \bar{x}_0 | \bar{n})^2. \quad (2)$$

First, the data is centered by subtracting the mean $\bar{x}_0 = \frac{1}{M}\sum_{i=1}^{M} \bar{x}_i$. Then, the normal vector $\bar{n}$ of the hyper plane is found using SVD on $\bar{x}_i$'s as the right singular vector (RSV) corresponding to the smallest singular value. Naturally, the other two RSVs span the TLS plane.

3) Identifying the Fitted Axes

The SVD that is used in the TLS fit does neither give out the axes in the same order as the time behavior implies nor is it guaranteed not to result in an axis pointing to the opposite direction than anticipated. To counteract this, the all the TLS axes are projected to all the "natural directions" of the loop structure. The so-called natural directions are defined as:

- the "forward-ponting" vector towards the apex of the loop structure (e.g. towards R-peak),
- a "left-pointing" average vector from the beginning to the apex of the loop, and
- a "up-pointing" cross-product vector orthogonal to the previous ones.

Finally, we then choose a reordering that maximizes the sum of the absolute values of the projections. In case the chosen projection length is negative, the corresponding TLS axis is reversed.

4) Finding the Optimal Rotation Matrix and Euler Angles

Let now X and Y be the two orthonormal 3-by-3 matrices that contain the TLS bases as column vectors, then the optimal rotation matrix between the two coordinate systems can be computed as

$$R = USV^T, \quad (3)$$

where $S = I$ if $\det(UV) = 1$. Otherwise, $\det(UV) = -1$, and $S = \mathrm{diag}(1, \ldots, 1, -1)$. S ensures that we obtain a true rotation, not a reflection. For derivation, see e.g. [14].

Further, the rotation matrix (3) can be decomposed into three subsequent rotations about the coordinate axes [15]. The corresponding rotation angles are dubbed as the Euler angles. It should be noted that they depend on the order of rotations. In the ZYX convention the rotation is performed first around the X-axis by φ radians, then around the Y-axis by θ radians and finally around the Z-axis by ψ radians.

5) Spatial Feature Extraction

To describe the shape of the loop structures, we define the following set of spatial features. The arc length (1) is already defined and calculated to accomplish equidistant interpolation. The ellipticity is defined as the ratio of the singular values σ_1 and σ_2 of the forward-pointing and the left-pointing axes, i.e.

$$e = \frac{\sigma_1}{\sigma_2}. \quad (4)$$

The singular values describe the major and minor axes of the elliptical distribution of the data points projected onto the plane. For circular loop structures, e is near 1. Moreover, flattened ones yield values smaller that one, but pointed ones result in values larger than one.

6) Goodness of plane fit (GF)

Finally, a measure for the goodness of the plane fit (GF) is defined as the ratio of energy contained in the subspace orthogonal to the plane, i.e.

$$GF = \frac{\sigma_3^2}{\sigma_1^2 + \sigma_2^2 + \sigma_3^2}. \quad (5)$$

For totally planar loop structures GF is 0, and the more three-dimensional the loop, the more positive is the GF value.

It should also be noted that the arc-length resampling affects the centroid of the data, and consequently, the spatial features described above.

B. The reference measure: PCA3

The parameter PCA3 of Acar *et al.* was used as a reference measure for the new GF parameter in determining the three-dimensionality of T-wave loop. PCA3 observes the projection of T-wave loop on a two-dimensional plane spanned by the first and the third component, see Eq.6.

$$\mathrm{PCA}_3 = \frac{\sigma_3}{\sigma_1} \times 100 \qquad (6)$$

Eigenvalue σ_i is associated with the *i*:th principal component. Computational details of the method have been previously described in detail by Acar *et al.* [10].

C. Dataset

The study group consisted of 24 healthy persons (age 44 +/- 13 years) and 52 patients who were recovering from an inferior of an inferior MI (age 63 +/- 15 years). All the patients had recovered from the first infarction and all reinfarctions were excluded. The data was recorded four to seven days after the heart failure. Based on the clinical findings and purpose of analysis by cardiac disorder, patients were grouped into two diagnostic categories: anterior MI, inferior MI. Other infarction types were excluded.

Digital 8-lead ECG data were recorded with a Welch Allyn Cardiocontrol BV digital ECG recorder (Welch Allyn Inc., Skaneateles Falls, USA) at the University Hospital of Oulu. All the measurements were done without the built-in digital filter of the ECG recorder. The sampling frequency was 600 Hz. During the measurements, the patients were lying on a bed. The skin was shaved and rubbed with sandpaper where the Blue Sensor R-00-S (Medicotest, Lstykke, Denmark) electrodes were placed at. Wavelet filtering was applied to ECG recordings to remove artefacts caused by muscle movement and power line interference. The coiflet wavelet (Coif5) of order 5 was used, because it has the lowest denoising error among Coiflet-functions with ECG data. [16,17]

III. RESULTS AND DISCUSSION

The results of the study are shown in Figures 2-4. In general, both measures of the non-planarity of T-wave loop had larger values among the patients with myocardial infarction compared to the healthy group. The parameter GF separated healthy group and "all MI patients" -group with p-value 0.002 and PCA3 with non-significant p-value 0.075 (Fig.2). Non-parametric Mann-Whitney test (SPSS software, version 14.0.1, SPSS Inc., Chicago, USA) was used as a statistical test. The null hypothesis was that the means of the groups are identical.

Furthermore, myocardial infarction patients were divided in two groups: anterior and inferior infarctions. The results between the three groups are illustrated in Figures 3-4. The difference in the non-planarity between healthy people and the patients was even clearer, when only anterior MI patients were included in patient group. Both GF (p=0.001) and PCA3 (p=0.016) separated healthy and anterior MI groups, while the p-value of GF was significantly better. P-values between healthy and inferior MI groups were 0.048 for GF and 0.66 for PCA3. In summary, GF parameter was able to differentiate the healthy group from both patient groups significantly better than PCA3.

The reason for that the GF performed so differently between the patient groups may be that patients with inferior MI have in general smaller functional and regional damages caused by infarction compared to anterior MI, and therefore the changes in ECG and VCG loops are also smaller and healthier with inferior MI patients.

PCA3 (p=0.008) differentiated between the locations of the myocardial infarction significantly, whereas GF (p=0.154) not, see Fig. 3 and 4. However, the specificity of PCA3 is poor since it confuses completely the healthy subjects and patients with inferior myocardial infarction.

In our new method the roundness of the loop did not affect to the planarity of the loop. For instance during dynamic ECG recordings, the total energy and the planarity of the loop may remain, but the roundness of the loop varies due to movements and breathing. In that case the value of the PCA3 also changes, because it is not related to the total energy, but only the first eigenvalue of the PCA. This risk has been eliminated in our method.

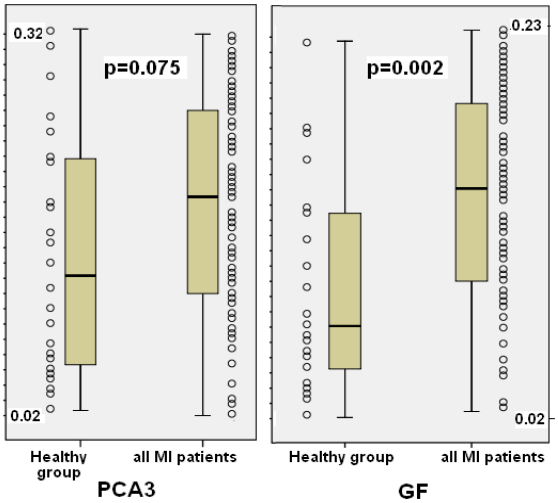

Figure 2. The distributions of the PCA3 and the GF -parameters and their p-values between healthy group and "all MI patients" -group.

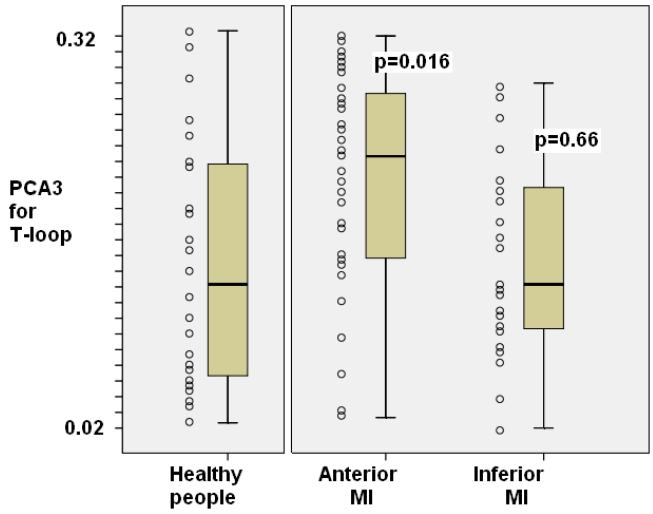

Figure 3. The distributions of PCA3 in healthy group and in anterior and inferior MI patients. The p-values are calculated between 1) healthy and anterior MI groups and 2) healthy and inferior MI groups.

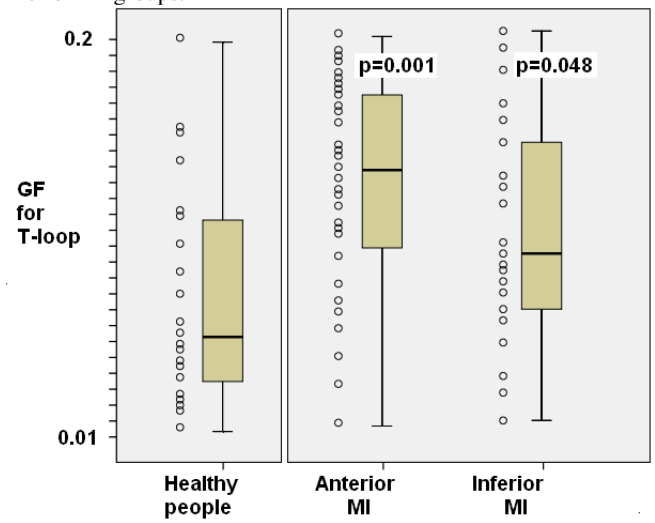

Figure 4. The distributions of GF in healthy group and in anterior and inferior MI patients. The p-values are calculated between 1) healthy and anterior MI groups and 2) healthy and inferior MI groups.

IV. CONCLUSION

New method for estimating the non-planarity of the VCG loop structures was introduced. The benefits include the robustness against external artefacts and inaccuracy of loop segmentation.

The non-planarity of T-wave loop was tested with ECG data, and it was shown to be significantly increased in patients with myocardial infarction compared to the healthy group. The new method separated healthy and patient groups with p-value 0.002 while PCA3 only with p-value 0.075. The new method was superior to PCA3 in separating the healthy patients from both infarction types.

In future, the method will be applied to larger patient data in order to confirm its performance and to test its power as a predictor of the mortality together with other PCA-based predictors.

REFERENCES

[1] S. G. Priori, D. W. Mortara, C. Napolitano, L. Diehl, V. Paganini, F. Cantu, G. Cantu, P. J. Schwartz, "Evaluation of the spatial aspects of T-wave complexity in the long-QT syndrome," *Circulation* vol. 96, pp. 3006-3012, 1997.

[2] P. M. Okin, R. B. Devereux, R. R. Fabsitz, E. T. Lee, J. M. Galloway, B. V. Howard, "Principal component analysis of the T wave and prediction of cardiovascular mortality in American Indians," *Circulation,* vol. 105, pp. 714-719, 2002.

[3] S. Severi, E. Grandi, G. Alessandrini, A. Santoro, S. Cavalcanti, "Principal Component Analysis of the T Wave: 24 Hour Monitoring of Repolarization Complexity in Dialysis Patients," *Computers in Cardiology,* vol. 33, pp. 701–704, 2006.

[4] M. Zabel, M. Malik, K. Hnatkova et al., "Analysis of T-wave morphology from the 12-lead electrocardiogram for prediction of long-term prognosis in male US veterans," *Circulation,* vol. 105, pp. 1066-, 2002.

[5] P. M. Rautaharju, C. Kooperberg, J. C. Larson, "Electrocardiographic predictors of incident congestive heart failure and all-cause mortality in postmenopausal women: The women's health initiative," *Circulation,* vol. 113, pp. 2481–489, 2006.

[6] F. Extramiana, A. Haggui, P. Maison-Blanche, R. Dubois, S. Takatsuki, P. Beaufils, A. Leenhardt, "T-Wave Morphology Parameters Based on Principal Component Analysis Reproducibility and Dependence on T–Offset Position", *Annals of Noninvasive Electrocardiology*, vol. 12, pp. 354-363, 2007.

[7] P. Rubel, J. Fayn, N. Mohsen et al., "New methods of quantitative assessment of the extent and significance of serial ECG changes of the repolarization phase," *Journal of Electrocardioly,* vol. 21 pp.(Suppl):S177–S181, 1988.

[8] J. Fayn, P. Rubel, "CAVIAR: A serial ECG processing system for the comparative analysis of VCGs and their interpretation with auto-reference to the patient," *Journal of Electrocardiology*, vol. 21, pp. (Suppl):S173—S176, 1988.

[9] F. Badilini, J. Fayn, P. Maison-Blance, A. Leenhardt, M. C. Forlini, C. P. Denjoy, P. J. Schwartz, "Quantitative aspects of ventricular repolarization: Relationship between three-dimentional T wave loop morphology and scalar QT dispersion," *Annals of Noninvasive Electrocardiology,*vol. 2, pp. 146-157, 1997.

[10] B. Acar, G. Yi, K. Hnatkova, et al., "Spatial, temporal and wavefront direction characteristics of 12-lead T-wave morphology," *Medical & biological engineering & computing,* vol. 37, 1999, pp. 574-584.

[11] K. Noponen, M. Karsikas & T. Seppänen, "A Method for Robustly Determining the Relative Orientation of Vectorcardiographic Loop Structures," in *World Congress 2009, 11th International Congress of the IUPESM*, Sept 7–12, Munich, Germany. (Submitted)

[12] F. N. Fritsch and R. E. Carlson, "Monotone Piecewise Cubic Interpolation," *SIAM J. Numerical Analysis*, vol. 17 , pp.238-246, 1980.

[13] J. Stoer, and R. Bulirsch : *Introduction to Numerical Analysis* (3rd ed.). Springer, New York, 2002.

[14] S. Umeyama S, "Least-squares estimation of transformation parameters between two point patterns*," IEEE Trans Pattern Anal Mach Intell*, vol. 13, pp. 376–380, 1991.

[15] P. Heckbert (ed.), *Graphics Gems IV*. Academic Press, San Diego, 1994.

[16] P. E. Tikkanen, "Nonlinear wavelet and wavelet packet denoising of electrocardiogram signal," *Biological cybernetics* vol. 80, pp. 259-267, 1999.

[17] L. Lehtola, M. Karsikas, M. Koskinen, H. Huikuri, and T. Seppänen, "Effects of noise and filtering on SVD-based morphological parameters of the T wave in the ECG", *Journal of Medical Engineering and Technology*, vol 32, pp. 400-407, 2008.